

Enhancing HEVC Compression: A Novel Algorithm for Swift and Efficient Intra Prediction

^{1*}M. N. Praphul, ²Dr. Aravinda H. S.

¹Research Scholar, Dept. of ECE, JSSATE,

²Professor, Dept. of ECE, JSSATE,

^{1,2}Affiliated to Visvesvaraya Technological University, Belagavi – 590018

Abstract: -High-Efficiency Video Coding (HEVC) represents the cutting-edge in video compression standards for high-resolution visual data. The prowess of HEVC lies in its utilization of prediction, capitalizing on signal redundancies to attain optimal compression efficiency. A key feature, the Intra-Picture prediction block, anticipates a block within the present frame by referencing information from adjacent blocks within that same frame. Nonetheless, this innovation introduces a significant surge in encoding complexity. Addressing this surge and reducing the computational demands of the coder becomes imperative. The present research introduces an innovative algorithm targeting mode decisions grounded on intra prediction. This algorithm assesses the texture intricacy of the coding unit and establishes an optimal threshold, enabling swift coding unit size selection. Subsequently, an enhanced search procedure minimizes the candidate modes of prediction. Culminating this approach, early termination gets implemented for rate-distortion optimized quantization (RDOQ) within Intra prediction. Findings indicate that the novel algorithm facilitates a reduction of approximately 40.9% in encoding duration.

Keywords: *High-Efficiency Video Coding (HEVC), Video Compression Standards, Intra-Picture Prediction, Encoding Complexity, Mode Decisions, Rate-Distortion Optimized Quantization (RDOQ).*

1. Introduction

In contemporary society, digital video stands as a pivotal tool in communication, entertainment, education, and information dissemination, exerting a substantial economic and socio-cultural influence. Throughout the initial decade of the 21st century, video's ascendancy as a primary information conduit - spanning platforms from digital television to Skype and from DVD to Blu-ray, inclusive of platforms like YouTube and Netflix - gained recognition. Given the vast data volumes intrinsic to digital video representation, compressing this data becomes essential, especially for feasible transmission, storage, and streaming.

The inherent structure of a digital video signal harbors considerable similarity and correlation among adjacent pixels and sequential frames. This structure predisposes the signal for compression, primarily through redundancy elimination or reduction. The phenomenon of chroma subsampling, where minimal visual disparities arise despite the subsampling, underscores this redundancy. Consequently, by subsampling, data rate reductions - synonymous with data compression - materialize. Beyond this, digital video signals exhibit multiple redundancy forms.

The process of digitization demands an extensive bit count to depict an image or video frame. Yet, the indispensable bit count for accurate representation might be notably diminished, attributed to the redundancy. Here, redundancy quantifies as the difference between one and the ratio of the minimal bit requirement for accurate image depiction to the actual bit allocation. For imagery abundant in spatial details, like a foliage scene, this constitutes 46%, whereas for images with lower detail gradations, such as facial representations, it

escalates to 74%. The primary objective of compression methodologies revolves around minimizing the bit requisition for frame representation by addressing this redundancy.

Delving deeper, spatial redundancy emerges due to correlations in both horizontal and vertical spatial dimensions among proximate pixel values within a consistent image or video frame - a phenomenon termed intra-picture correlation. Adjacent pixels within video frames frequently exhibit pronounced similarity, especially when segregating frames into luma and chroma components. Segmenting a frame into diminutive pixel blocks capitalizes on these correlations, given the heightened correlation within individual blocks. Essentially, within confined frame segments, spatial dimension alterations manifest at subdued rates. Such a configuration indicates that, within a video frame's frequency-domain portrayal, energy predominantly congregates in the low-frequency domain, with high-frequency transitions being an exception.

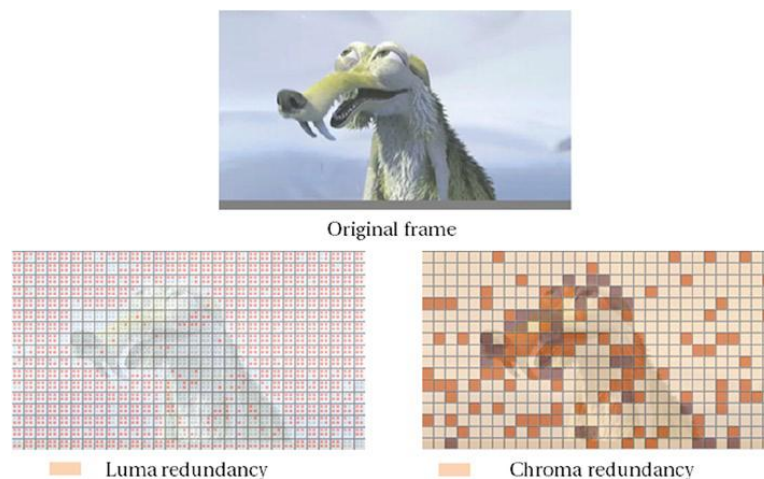


Figure 1: Illustration of Spatial Redundancy Observed within an Image or Video Frame.

Figure 1 illustrates the manifestation of spatial redundancy within a video frame. The degree of redundancy inherent in a frame is contingent upon multiple factors. Parameters such as the sampling rate, quantization levels, and inherent source or sensor noise exert influence on the compression feasibility. Elevated sampling rates coupled with diminished quantization levels and minimal noise translate to an augmented pixel-to-pixel correlation, thereby amplifying the spatial redundancy that can be harnessed.

The High-Efficiency Video Coding (HEVC), recognized as the H.265 standard (ISO/IEC 23008-2), emerged as the preeminent joint video coding standard in 2013, receiving endorsement from the ITU-T Video Coding Experts Group (VCEG) and the ISO/IEC Moving Picture Experts Group (MPEG) standardization entities. This standard succeeds its predecessor, the AVC or H.264, which was delineated by the collaborative efforts of MPEG and VCEG under the Joint Collaborative Team on Video Coding (JCT-VC). The impetus behind HEVC arose from the escalating demand for advanced resolution videos, spanning high-definition (HD, 1920×1080) to ultra-high definition (UHD, $4k \times 2k$) and beyond. HEVC primarily addresses dual challenges: the amplification of video resolution and the augmented adoption of parallel processing architectures. The foundational objective of the HEVC algorithm centers on attaining a compression efficiency that doubles the capability of AVC.

Within the HEVC framework, the optimal intra prediction mode undergoes identification by implementing rate-distortion optimization (RDO) across every conceivable mode and all coding unit (CU) dimensions [03]. Such an approach culminates in a significant computational burden. In this research, a preprocessing maneuver gets deployed to diminish the potential intra prediction modes for a CU, directing the RDO towards a restricted mode ensemble. This document introduces an accelerated mode decision technique for HEVC, delivering substantial computational savings. Through the proposed methodology, from an initial set of 33 modes, a mere 9 modes prevail, procured post the RMD procedure, grounded on the interrelationships among angular modes, thereby reducing the mode count.

2. Literature Survey

Kalali et al. [01] introduced a method aiming to diminish computational demands during intra-prediction in an HEVC decoder. Concurrently, a high-performance hardware design catering to 4x4 and 8x8 angular prediction modes was conceptualized using Verilog HDL. This design underwent validation on a Xilinx Virtex 6 FPGA, catering to Full HD resolutions of 1920x1080 and 1280x720. The innovation resulted in a commendable 42% decline in energy consumption during HEVC decoding's intra-prediction phase.

Abramowski et al. [02] showcased a hardware architecture tailored for intra-prediction within an HEVC encoder. This construct accommodated all directional modes and all Prediction Unit (PU) dimensions. A noteworthy modification involved substituting registers with a double-clocked RAM, designated for reference sample access. Such an alteration culminated in a minimized register utilization. The design also incorporated features allowing the bypass of specific prediction modes and PU sizes. The design's blueprint was articulated using VHDL and underwent synthesis via TSMC 0.13 μ m technology, demonstrating its prowess in real-time processing of 1080p video sequences. This endeavor received further expansion in [07], addressing the high resource consumption challenge. Analyses revealed that a significant chunk of computational complexity emanated from 4x4 Prediction Units (PUs). Thus, a dedicated processing path was allocated to this PU dimension. Comprehensive implementations on both FPGA and ASIC platforms were presented.

Kammoun et al. [03] delineated an optimized hardware accommodating all directional modes of 4x4 intra-prediction in HEVC. The architectural design underwent simulation and synthesis with TSMC 0.18 μ m technology and witnessed an implementation on a Xilinx Virtex 6 FPGA board. The hardware blueprint was crafted using VHDL in tandem with the ModelSim tool.

Jiang et al. [04] set forth a unified and streamlined hardware architecture dedicated to intra-prediction within HEVC. This architecture encompassed all 35 intra-prediction modes for every PU size. A novel feature of this design was the unified reference sample indexing system, eliminating the need for reference sample reconfigurations. The entire design was articulated in VHDL and materialized on a Xilinx Virtex 5 FPGA. Notably, this innovation led to a reduction in both hardware resource demands and dynamic power consumption.

Lastly, Abdellah et al. [05] realized an HEVC intra-prediction for 4x4 on a Xilinx Spartan-3E FPGA board. This hardware predominantly operated using only DC and angular modes for intra-prediction, with its design formulated in VHDL.

3. Methodology

All video coding protocols adhere to a consistent, traditional codec framework. This framework bifurcates into two primary segments: 1) the encoder and 2) the decoder.

Delving into the encoder segment, as depicted in the proposed methodology's architecture (Figure 2), every individual frame undergoes segmentation into uniformly sized picture blocks termed as macroblocks. Within the context of HEVC, these picture blocks receive the nomenclature of coding tree units (CTU). After this partitioning, each unit undergoes a prediction procedure, specifically the intra-frame prediction. The ensuing outcome of this prediction phase gets subtracted from the original picture block. Progressing further, the resulting residual undergoes transformation through the Discrete Cosine Transform, followed by quantization. The terminal phase of the encoding sequence witnesses the transformed output, prediction details, mode specifics, and headers being processed by an entropy encoder.

Conversely, the decoder's architecture mirrors its encoder counterpart, executing inverse functionalities. Each component of the encoder finds its antithesis in the decoder, ensuring the reconstruction of the original picture on the communication's receiving end.

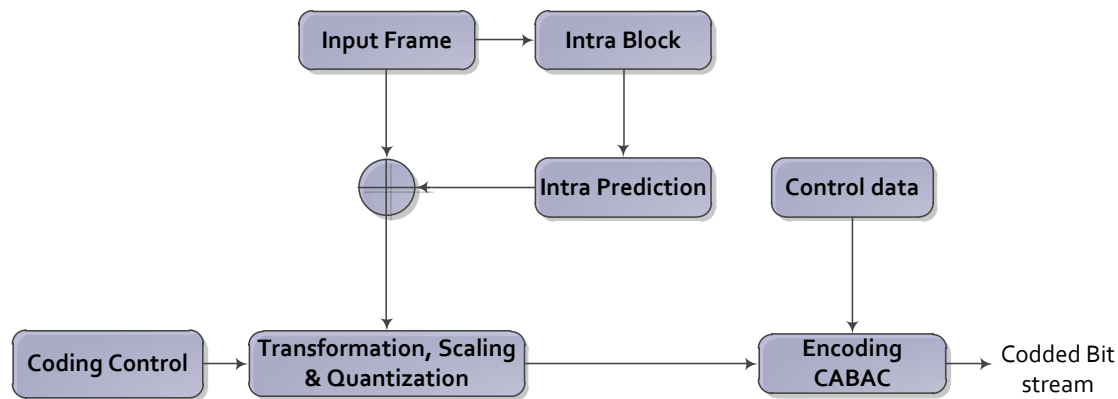


Figure 2: Schematic Representation of the Proposed System's Architecture.

3.1 Picture Structure and Partition

The High-Efficiency Video Coding (HEVC) employs the YCbCr color space for articulating color video signals. Within this color space:

- Y represents luminance, signifying the brightness of an image.
- Cb stands for blue chrominance, capturing the distinction between blue and luma ($B - Y$).
- Cr denotes red chrominance, highlighting the difference between red and luma ($R - Y$).

In its foundational design, HEVC utilizes an 8-bit precision to depict both input and output data. However, it's worth noting that enhancements to the standard are underway, aiming to accommodate increased bit depths. Given that the human visual system exhibits heightened sensitivity towards luma over chroma components, the initial iteration of HEVC exclusively endorses a 4:2:0 chroma subsampling. This configuration implies that each chroma component retains a mere one-fourth of the luma component's sample count.

Within the HEVC schema, the coding tree unit (CTU), synonymous with the largest coding unit (LCU), emerges as a pivotal structure. It encompasses a luma coding tree block (CTB), associated chroma CTBs, and pertinent syntax elements. Within the realm of a CTU, the dimensions of the luma block can span 16×16 , 32×32 , or 64×64 , as delineated in the bitstream sequence parameter set. To facilitate granular processing, CTUs can undergo further segmentation into diminutive square blocks, orchestrated through a tree configuration complemented by quad-tree signaling. This quad-tree demarcates the coding units (CU), which underpin the prediction and transformation processes. During the encoding phase, coding units within a coding tree block undergo a Z-order traversal. Figure 3 provides a visual representation, illustrating the potential segmentation of a 64×64 CTB into CBS.

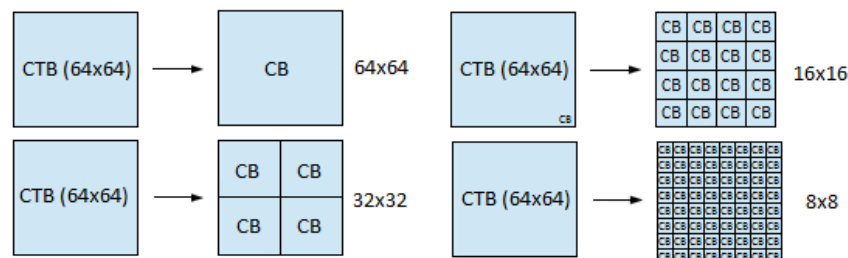


Figure 3: Sequential Arrangement of a 64×64 CTB.

In the HEVC framework, the coding unit (CU) emerges as the foundational unit for prediction, with its prediction derived from previously encoded data. As depicted in Figure 4, a CU is comprised of three coding blocks (CBs) representing Y (luma), Cb (blue chrominance), and Cr (red chrominance), along with their correlated syntax elements.

Within a CU:

- There exists one luma (Y) coding block and two chroma (Cb and Cr) coding blocks.
- These blocks can undergo further subdivisions in size and can derive predictions from their respective prediction blocks (PB), contingent on the specific prediction modality.
- HEVC boasts versatility in PB sizes, accommodating dimensions that span from as large as 64×64 to as minute as 4×4 samples.
- The prediction's residual, following the prediction process, is encoded leveraging the transform unit (TU) tree configuration.

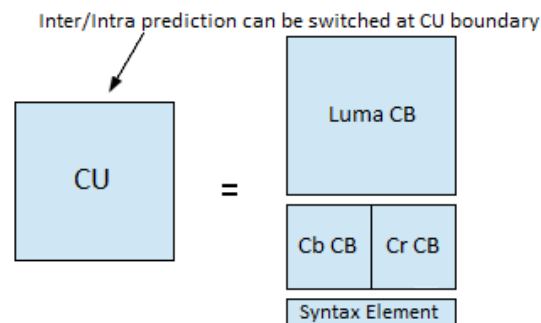


Figure 4: Composition of a CU Featuring Three CBs and Corresponding Syntax Elements.

In the context of HEVC, the residual derived from either the luma or chroma coding block might either mirror the dimensions of the associated transform block (TB) or undergo further segmentation into more compact transform blocks. It's pivotal to note that transform blocks adhere to a strict square geometry, with permissible sizes being 4×4 , 8×8 , 16×16 , and 32×32 .

For the 4×4 transform specific to intra-picture prediction residuals, the standard not only stipulates the conventional DCT-based integer transform but also designates an alternative: an integer transform rooted in a variant of the discrete sine transform (DST).

This intricate quad-tree configuration, integral to HEVC's design, is widely acknowledged as the pivotal factor amplifying HEVC's coding efficiency, especially when juxtaposed against its predecessor, AVC.

3.2 Intra-prediction

In the realm of HEVC, intra-picture prediction capitalizes on previously decoded boundary samples from spatially proximate image data within an identical picture to forecast a forthcoming prediction block (PB). Consequently, the inaugural picture of a video sequence—as well as the first picture at each distinct clean random-access juncture within a video sequence—is encoded exclusively through intra-picture prediction.

When considering an intra-predicted coding unit (CU), it can undergo bifurcation into PBs in two distinct modalities:

1. The dimensions of the PB mirror that of the CB.
2. The CB is further segmented into four reduced PBs. Notably, this latter scenario is exclusively permissible for the smallest 8×8 CUs. Within this context, a specific flag indicates if the CB has been divided into four 4×4 PBs, with each PB possessing its unique intra prediction mode.

HEVC exhibits versatility with 35 distinct intra modes tailored for PB prediction, a substantial enhancement from the eight modes found in H.265/AVC. These modes encompass:

DC Prediction: Here, every sample within the PB is calculated as the average of the boundary samples from adjacent blocks.

Planar Prediction: Within this mode, each PB sample is ascertained by presuming an amplitude surface characterized by horizontal and vertical gradients, both derived from the boundary samples of the neighboring blocks.

Directional Prediction: This mode boasts 33 unique directional orientations. For each PB sample, its value is determined by extrapolating from the boundary samples of the adjoining blocks.

3.3 Transform, Scaling, and Quantization

In the HEVC framework, the residual signal from intra-prediction—a differential measure between the original block and its anticipated counterpart—undergoes a transformation process, leveraging block transforms grounded in the Discrete Cosine Transform (DCT) or Discrete Sine Transform (DST). Notably, the DST is exclusively employed for intra-predicted 4x4 CUs.

This transformative process serves a dual purpose. Firstly, it transitions the residual signal into the frequency domain. Secondly, this shift facilitates the decorrelation and compaction of the underlying information. In terms of transform dimensions, HEVC encompasses four standard sizes: 4x4, 8x8, 16x16, and 32x32.

To achieve this transformation, each coding block (CB) can be systematically subdivided into Transform Blocks (TBs). This subdivision adheres to the quad-tree methodology, as graphically represented in Figure 5, analogous to the CTB partitioning—this process earns the moniker "residual quadtree." The maximum permissible TB dimension aligns with the CB's size.

Delving into the specifics:

- For a luma CB of dimensions $M * M$, a flag discerns if it gets segmented into four blocks, each with dimensions $\frac{M}{2} * \frac{M}{2}$.
- Chroma CBs, in contrast, adopt dimensions half that of their luma TB counterparts. Consequently, the minimum sanctioned Transform Unit (TU) size remains fixed at 4x4.

To illustrate, consider a 16x16 CU. It could comprise three 8x8 TUs and an additional four 4x4 TUs. For every luma TU, a corresponding chroma TU exists, with its size being a mere quarter of the luma TU's size. To contextualize, a 16x16 luma TU would be accompanied by a pair of 8x8 chroma TUs.

In the intricate realm of intra-prediction, the decoded samples from spatially proximate TBs serve as the foundational reference data.

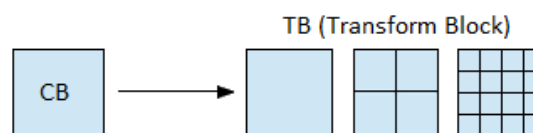


Figure 5: Visualization of the Transform Block Structure.

3.4 Entropy Coding

The residual data, post-processing, undergoes a structured rearrangement either via zigzag scanning or alternate field scanning. This data is then encoded employing context-adaptive binary arithmetic codes (CABAC). At its core, CABAC utilizes an adaptive binary arithmetic coder. This coder, post the encoding of every individual symbol, updates the probability estimate, facilitating adaptation in line with the context.

The CABAC entropy coding process can be demarcated into three pivotal stages:

1. Binarization:

- At this juncture, non-binary symbols, which can be anything from transform coefficients to motion vectors, undergo a unique mapping to yield a binary sequence, prepping it for arithmetic coding.

- Conceptually, this mapping mirrors the process of translating a data symbol into a variable-length code. However, an additional layer of encoding is imposed on this binary code by the arithmetic coder prior to its transmission.

2. Context Modeling:

- This stage is dedicated to the selection of a probability model for the binarized symbol, termed the context model. The choice of this model is contingent on the syntax elements encoded previously.

3. Binary Arithmetic Coding:

- Here, the arithmetic coder is tasked with encoding each element. This encoding adheres to the context model selected in the previous stage.
- Post encoding, the model undergoes an update to reflect the latest encoded data.

This intricate CABAC process ensures efficient data representation and compression, optimizing the data for transmission.

3.5 Proposed Algorithm for Optimal Mode Decision

In the context of video encoding, multiple intra prediction modes are available, from which a singular mode is selected and subsequently encoded in the bitstream. The Advanced Video Coding (AVC) standard delineates nine intra prediction modes for both 4×4 and 8×8 luma blocks, accompanied by four modes for a 16×16 luma block, and an additional four modes specific to each chroma block.

The methodology proposed in this study offers a comprehensive approach, taking into account both Coding Unit (CU) and Prediction Unit (PU) size or mode decision algorithms:

1. CU Partition:

- Here, the texture characteristic of the CU undergoes analysis. This analysis determines if further segmentation of the current CU is warranted.

2. PU Partition:

This segment leverages several techniques:

- **Down-sampling Prediction:** Aims to minimize computational overhead.
- **Similar Three-step Search:** A method to optimize the search process.
- **Early Termination for Intra Prediction:** A strategy to swiftly eliminate non-viable modes, thereby accelerating the intra prediction phase.

The intricacies of the entire process are as follows:

Central to the proposed algorithm is the adoption of a down-sampling technique. This approach aims to not only reduce computational complexity but also to filter out noise, thereby enhancing the clarity and accuracy of predictions. As depicted in Figure 6, the current CU is subjected to a 2:1 down-sampling filter. This filter employs a simplistic averaging operator, applied both horizontally (2:1 ratio) and vertically (2:1 ratio). It's noteworthy that CUs of varying dimensions undergo analogous operations, ensuring consistency across the board.

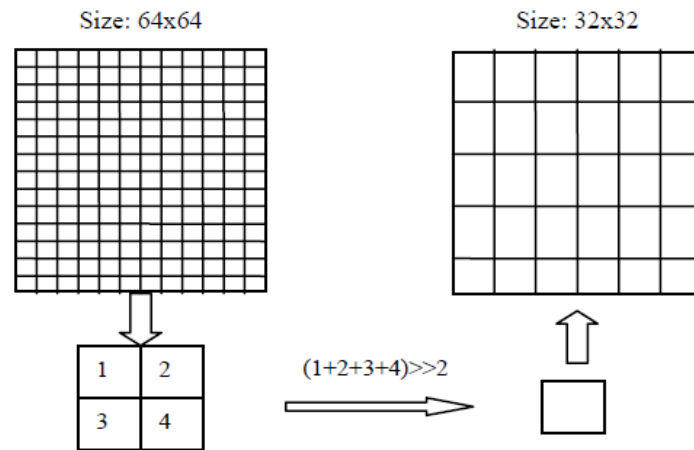


Figure 6: Down-sampling Process Using Simple Averaging on a 64x64 CU.

After the down-sampling process, the complexity of the original LCU can be quantified through its variance. This variance is mathematically represented as:

$$E_{\text{com}} = \sum_{i=0}^{N-1} \sum_{j=0}^{N-1} \left[p(i,j) - \frac{1}{N^2} \sum_{i=0}^{N-1} \sum_{j=0}^{N-1} p(i,j) \right]^2 \quad (1)$$

Where:

- E_{com} symbolizes the texture complexity.
- N denotes the size of the current CU.
- $p(i,j)$ represents the pixel value, and (i,j) specifies its coordinate within the CU.

Upon calculating the texture, two threshold values are established to balance coding quality and complexity reduction, denoted as *Thre1* and *Thre2*. The following conditions are applied:

1. If the computed complexity surpasses *Thre1*, the CU undergoes splitting.
2. If the complexity is less than *Thre2*, the CU is deemed optimal.
3. For complexities that lie between *Thre1* and *Thre2*, the methodology adheres to the guidelines established in the HEVC reference software.

In the HEVC reference software, selecting the optimal model from 35 modes introduces considerable computational complexities. This research introduces an algorithm tailored for mode decisions aimed at minimizing these complexities. The algorithm unfolds in two distinct stages:

1. The initial phase involves computing the Sum of Absolute Differences (SAD) using a down-sampling approach. Subsequently, a similar three-step search algorithm is deployed to exclude redundant modes.
2. The subsequent phase is centered on the early termination of Rate-Distortion Optimization (RDO).

A comprehensive breakdown of the algorithm's operations is provided in the subsequent sections. The schematic flow of the algorithm is visually represented in Figure 7.

Algorithm of Optimal Mode Decision

Inputs: Input Frames

Output: Optimal Mode Detection

The algorithmic approach detailed aims to efficiently identify optimal prediction modes from a set of 35 possibilities, reducing computational complexity. Here's a clearer and more structured presentation of the procedure:

Step.1 Initial Candidate Creation:

- Start by constructing an initial candidate list, $S1$, from the 35 prediction modes: $S1 = \{0, 1, 2, 6, 10, 14, 18, 22, 26, 30, 34\}$.
- From $S1$, select the 5 most optimal modes based on the Sum of Absolute Differences (SAD). Let's represent these as $S2 = \{0, 2, 10, 18, 34\}$.

Step.2 Three-Step Algorithm Application:

- Firstly, expand the list $S2$. The modes that are 2-distance neighbors of $S2$ are represented by $S3 = \{4, 12, 20, 32\}$ (with modes 0 and 1 treated distinctively).
- By assessing $S1$, $S2$, and $S3$, derive the optimal modes, represented as $S4 = \{6, 14, 22\}$.
- Presuming the modes of the upper and left Prediction Units (PUs) are $S5 = \{1, 4\}$, cross-check against all previous lists ($S1$ through $S4$) to derive the two most optimal modes, represented as $S6 = \{4, 6\}$.

Step.3 Refining Candidate Modes:

- For $S6$, the 1-distance neighbors are represented by $S7 = \{3, 5, 7\}$.
- The best K modes, intended for a full Rate-Distortion Optimized Quantization (RDOQ), are selected by scrutinizing the lists from $S1$ through $S7$. Assuming $K = 3$, the modes are $\{3, 5, 6\}$.
- Furthermore, if the minimal cost of modes is C_{\min} (where C_{\min} represents the cost of the mode with the smallest value), and the cost of mode m surpasses a weighted C_{\min} , given by $C_{\{m\}} > \alpha C_{\min}$, then mode m won't undergo a full RDOQ. If $C_{\{m\}} < \alpha C_{\min}$ and $m - \text{text}\{\min\} > 3$, then mode m is skipped. However, if $m - \text{text}\{\min\} < 3$, the standard HEVC reference software algorithm is applied. All other modes are processed in a similar manner.

This methodology systematically refines the mode selection, ensuring that only the most pertinent modes undergo comprehensive processing, thus economizing computational resources.

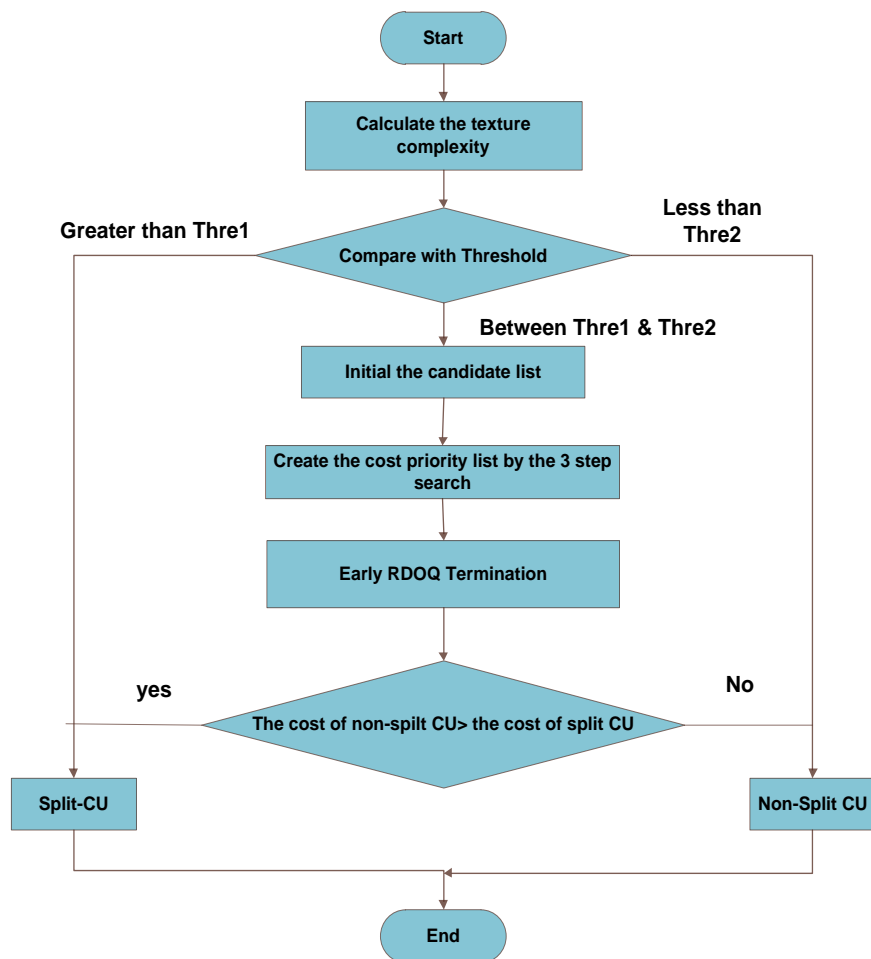


Figure 7: Schematic Flowchart Illustrating the Proposed Algorithm.

4. Experimental Results

A comprehensive set of experiments was conducted to gauge the effectiveness and computational intricacies of the intra mode selection algorithm proposed in this study.

During the initial phase, the encoder generated a prediction for the current Prediction Unit (PU). This prediction was based on extrapolating values sourced from reference pixels of adjacent PUs. Notably, only half of the typical angular modes were employed, resulting in the utilization of 9 modes as opposed to the standard 35. Subsequent to this, the costs associated with the remaining modes were calculated, leveraging the mean costs of two proximate modes. The Rate-Distortion Optimization (RDO) function was then applied to N selected modes that showcased the lowest cost values, in addition to potential modes extracted from neighboring blocks.

The interrelations among the angular modes played a pivotal role in the next phase. Prior to initiating the RDO operations, certain modes identified in the first phase were excluded. This strategic omission aimed to curtail both the encoding duration and the computational complexities inherently associated with intra prediction.

All frames underwent encoding via the context adaptive binary arithmetic coding (CABAC) entropy, with the sample adaptive offset (SAO) feature activated. To quantify the efficacy of the proposed methodology, several metrics were employed: PSNR (Before Interpolation), PSNR (After Interpolation), and Bitrate.

The entire experimental framework was executed across ten distinct sequences, spanning two classes. These experiments employed varying Quantization Parameters (QPs), namely 20, 26, 30, 36, and 40. The results of these evaluations are visually represented in Figures 8 and 9.

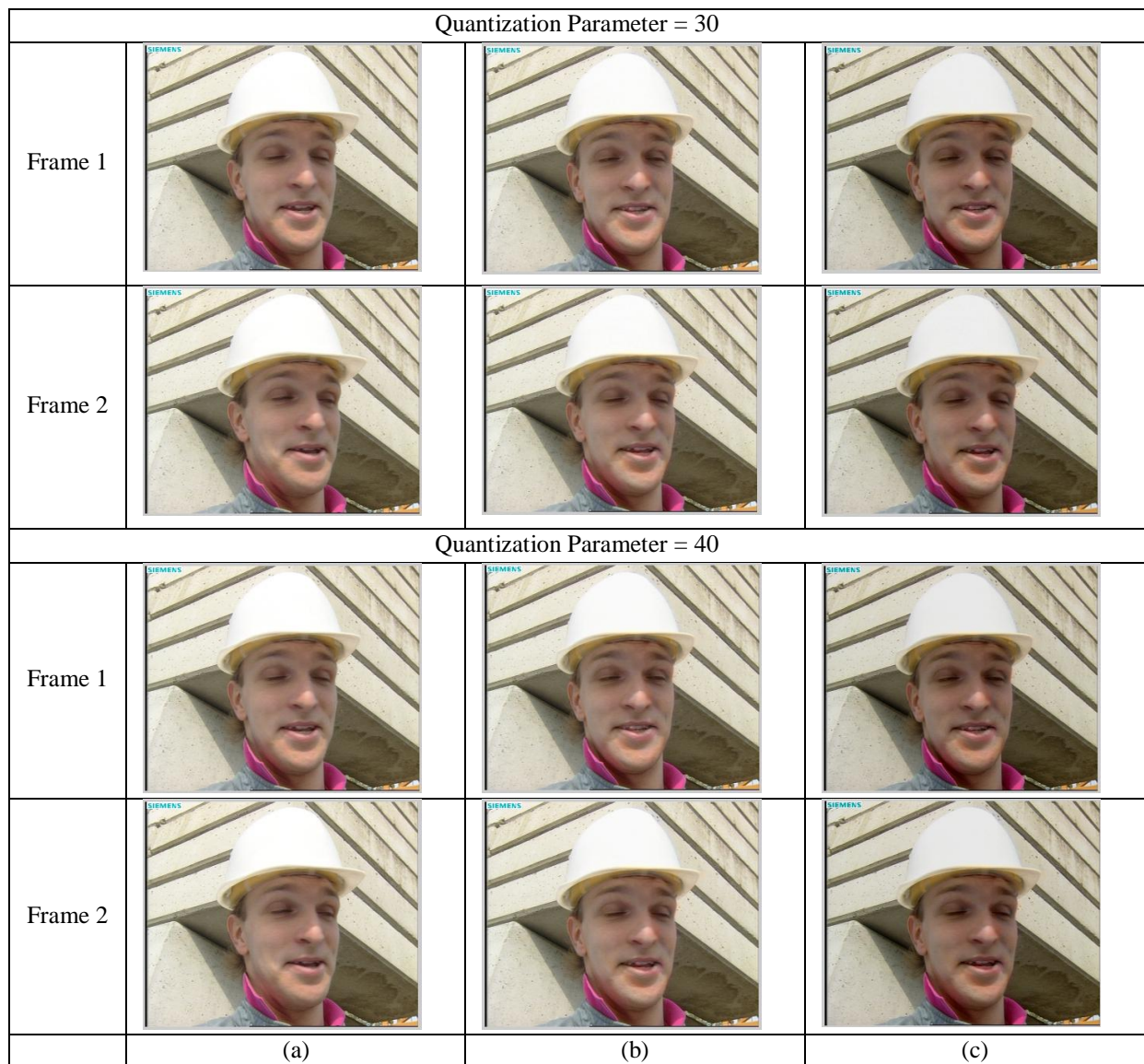


Figure 8: Comparative Frames - (a) Original Input Frame; (b) Resulting Predicted Frame; (c) Subsequent Interpolated Frame.



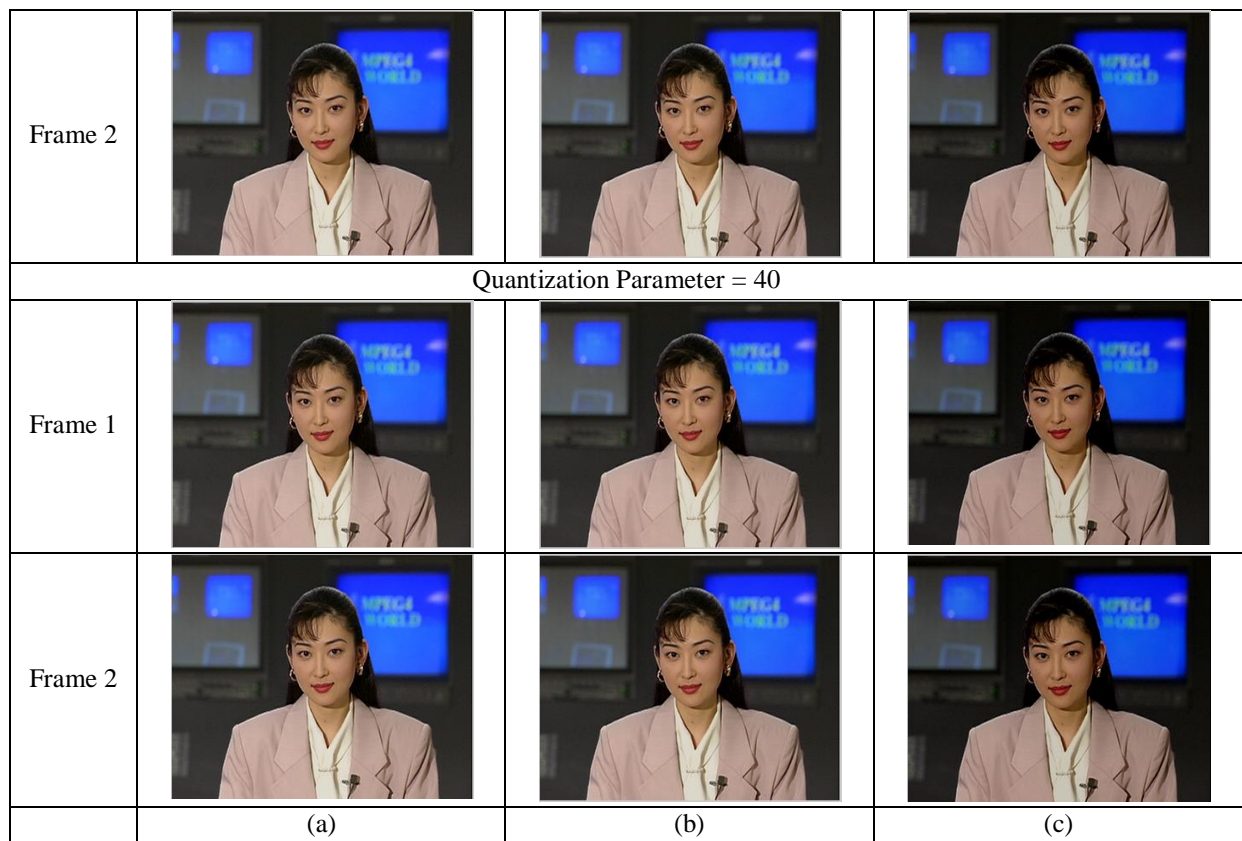


Figure 9: Frame Analysis - (a) Initial Input Frame; (b) Corresponding Predicted Frame; (c) Final Interpolated Frame.

The Peak Signal to Noise Ratio (PSNR) stands as the predominant metric employed to evaluate the quality of frames processed through lossy compression codecs. This measure offers a comparative analysis between the original frame and its reconstructed counterpart post-compression. PSNR quantifies the mean squared error (MSE) between the original and the reconstructed video frame, representing this error on a logarithmic scale in relation to the squared magnitude of the maximum possible signal value inherent in the frame.

Table I delineates the performance analysis of the proposed system across varied Quantization Parameter (QP) values. Furthermore, Figure 10 visually portrays the average PSNR and Bit Rate metrics of the proposed system (with a constant bit rate) juxtaposed against an existing system.

$$PSNR = 10 \log_{10} \frac{(2^{bit-length} - 1)^2}{MSE} \quad (2)$$

$$MSE = \frac{1}{M \cdot N} \sum_{i=0}^{M-1} \sum_{j=0}^{N-1} (OriginalBlock(i, j) - ReconstructedBlock(i, j))^2 \quad (3)$$

Table 1: Performance Analysis of the Proposed System for Different QP Value

	QP		PSNR (Before Interpolation)	PSNR (After Interpolation)	Bit rate
Foreman_Video	21	Frame 01	47.431	50.631	1880.282
		Frame 02	47.425	50.601	1777.329
	27	Frame 01	43.868	47.899	1228.641
		Frame 02	43.868	47.881	1171.485

	31	Frame 01	40.868	43.253	878.516
		Frame 02	40.869	43.245	843.126
	37	Frame 01	35.267	37.868	582.719
		Frame 02	35.251	37.869	559.313
	41	Frame 01	31.619	33.267	451.094
		Frame 02	31.595	33.251	431.891
Akiyo_Video	21	Frame 01	49.726	61.483	457.047
		Frame 02	49.743	61.696	446.813
	27	Frame 01	44.893	54.993	343.985
		Frame 02	44.898	55.076	336.907
	31	Frame 01	41.893	46.574	287.047
		Frame 02	41.898	46.597	279.422
	37	Frame 01	35.032	38.893	232.907
		Frame 02	35.029	38.898	226.485
	41	Frame 01	31.151	33.032	205.157
		Frame 02	31.149	33.029	199.469

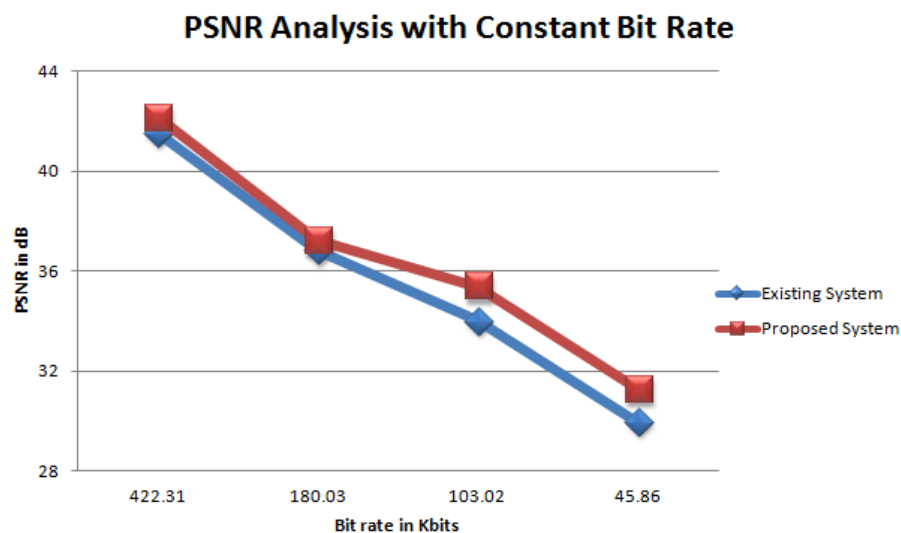


Figure 10: Comparative Graph Showcasing Average PSNR and Bit Rate between the Proposed System (With Consistent Bit Rate) and the Existing System.

5. Conclusion

The High Efficient Video Coding (HEVC) standard has risen to prominence, catering to the escalating demand for superior coding efficiency and enhanced video content compression. Thus, a paramount objective is to curtail this computational complexity while retaining the compression efficacy, primarily by refining the Intra-Picture prediction block.

To assess the performance, the BD-rate is derived from the PSNR and bit rate metrics, with optimal outcomes being ascertained through a linear decision boundary. One notable advantage of the proposed methodology is the diminished computational complexity. This is evident from the reduced number of Sum of Absolute Differences (SAD) operations when contrasted with the conventional HEVC approach.

Empirical results validate the efficacy of the proposed strategy. Specifically, employing a quadratic decision boundary and amalgamating three features, the proposed system can encode two video sequences with an

average operational reduction of 16.5% compared to the conventional HEVC. This operational efficiency is achieved at the expense of marginal compression efficiency losses, as quantified by the BD-rate.

Reference

- [1] E. Kalali, Y. Adibelli, and I. Hamzaoglu, "A high performance and low energy intra-prediction hardware for high-efficiency video coding," in Field Programmable Logic and Applications (FPL), 2012 22nd International Conference on, 2012, pp. 719-722.
- [2] A. Abramowski and G. Pastuszak, "A novel intra-prediction architecture for the hardware HEVC encoder," in Digital System Design (DSD), 2013 Euromicro Conference on, 2013, pp. 429-436.
- [3] A. Abramowski and G. Pastuszak, "A double-path intra-prediction architecture for the hardware H. 265/HEVC encoder," in Design and Diagnostics of Electronic Circuits & Systems, 17th International Symposium on, 2014, pp. 27-32.
- [4] M. Kammoun, A. Ben Atitallah, and N. Masmoudi, "An optimized hardware architecture for intra-prediction for HEVC," in Image Processing, Applications and Systems Conference (IPAS), 2014 First International, 2014, pp. 1-5.
- [5] Y. Jiang, D. Llamocca, M. Pattichis, and G. Esakki, "A unified and pipelined hardware architecture for implementing intra-prediction in HEVC," in Image Analysis and Interpretation (SSIAI), 2014 IEEE Southwest Symposium on, 2014, pp. 29-32. 84 84
- [6] S. Abdellah, S. Youcef, and D. Lamine, "Implementation of HEVC intra 4×4 predictions on FPGA," in Science and Information Conference (SAI), 2015, 2015, pp. 1160-1164.
- [7] J. Vanne and T. D. Hämmäläinen, "Panu Sjövall High-Level Synthesis Of Hevc Intra-Prediction On Fpga."
- [8] M. Fingeroff, High-level synthesis blue book: Xlibris Corporation, 2010.
- [9] An open-source HEVC encoder. Available: <https://github.com/ultravideo/kvazaar>
- [10] I. H. Ercan Kalali, "FPGA Implementation of HEVC Intra-prediction Using High-Level Synthesis," presented at the International Conference on Consumer Electronics, Berlin, 2016.
- [11] Nouripayam and N. Sheikhipoor, "HEVC (H. 265) Intra-Frame prediction implementation Using MATLAB," 2014.
- [12] G. J. Sullivan, J. R. Ohm, W. J. Han, and T. Wiegand, "Overview of the High-Efficiency Video Coding (HEVC) Standard," IEEE Transactions on Circuits and Systems for Video Technology, vol. 22, pp. 1649-1668, 2012.

Bibliography



Praphul M N, Research Scholar in the Department of E&CE, JSSATE, Bangalore. He received his B.E degree in Electronics and Communication Engineering and obtained M.Tech degree in VLSI and Embedded Systems from Visvesvaraya Technological University, Belagavi. He worked as an Assistant Professor in the Department of Electronics & Communication Engineering at MVJ College of Engineering, Bangalore. His research interest includes VLSI and Signal Processing.



Dr. Aravinda H. S. holds the position of Professor in the Department of Electronics & Communication Engineering at JSS Academy of Technical Education, Bangalore. This scholar completed a B.E. Degree in Electronics & Communication Engineering from Bangalore University in 1996. Post-graduation was achieved from Mysore University in 1999. A Ph.D. on the subject of "Fault tolerance Measurements Techniques of Acoustic Spectrum" was awarded by VTU during 2012-2013. Primary research interests include Fault Tolerance, Signal Processing, and Image Processing. With 24 years of experience in teaching engineering for UG & PG courses, more than 50 papers have been published in both international and national journals and conferences. Additionally, Dr. Aravinda H. S. reviews for six national and international journals.